

Laser-Sustained Plasmas in Forced Convective Argon Flow, Part II: Comparison of Numerical Model with Experiment

San-Mou Jeng,* Dennis R. Keefer,† Richard Welle,‡ and Carroll E. Peters§
University of Tennessee Space Institute, Tullahoma, Tennessee

A two-dimensional laser-sustained plasma model, which is based on the laminar, Navier-Stokes equations for the flow and geometric ray tracing for the laser beam, has been evaluated and compared with existing experimental results for a wide range of forced convective argon flows. The influence of gas inlet velocity, gas pressure, laser power, and focusing geometry on the structure of the plasma was examined. The model agreed well with the existing experimental data in both global structure and detailed temperature distribution, particularly for static pressures greater than 2 atm. It was found that the diffusion approximation for the optically thick portion of the thermal radiation was not adequate for low-pressure (less than 2 atm) plasmas and that the radiation-induced thermal conductivity had to be adjusted in order to obtain agreement between the model calculations and experimental results. The present model calculations were also compared with a recently published semi-two-dimensional model and the results indicate that the existing one-dimensional and semi-two-dimensional models do not provide adequate solutions for the laser-sustained plasma.

Nomenclature

c_p	= specific heat at constant pressure, J/kg·K
h	= specific enthalpy, J/kg
I	= laser intensity, W/m ²
k	= intrinsic thermal conductivity, W/m·K
k_{eff}	= effective thermal conductivity, W/m·K
k_{rad}	= radiation-induced thermal conductivity, W/m·K
\dot{q}_{rad}	= radiation heat loss, J/m ³ ·s
r	= radius, m
s	= distance along the laser ray, m
u	= axial velocity, m/s
v	= radial velocity, m/s
x	= axial distance, m
y	= radial distance, m
α	= absorption coefficient at 10.6 μm wavelength, 1/m
μ	= viscosity, kg/m·s
ρ	= density, kg/m ³

Introduction

THE main objective of the present investigation was to evaluate a proposed new model¹ for predicting both the global and detailed structure of laser-sustained plasmas (LSP) under various flow conditions and optical geometries. Although the low-molecular-weight hydrogen is the best propellant for laser thermal propulsion, there is very little hydrogen LSP data available at present. Therefore, this investigation was limited to axisymmetric LSP in flowing argon, since we have made detailed measurements of their

structure in our laboratory.^{2,3} A separate theoretical study, using a similar model, for the hydrogen LSP can be found in Ref. 4.

It has been pointed out^{5,6} that a basic understanding of the interaction between a high-power laser beam and a plasma is needed and that the following questions must be answered before designing a laser thermal propulsion thruster. How can the position and size of the LSP, which are clearly related to the size and shape of the absorption chamber, be controlled? How can the power conversion efficiency from laser energy to propellant thermal energy be maximized? How can damage to the absorption chamber from the high-power laser beam and the high-temperature plasma be avoided? In order to answer these questions, experiments with laboratory-sized LSP under various flow conditions and optical geometries have been performed.^{2,3} However, a theoretical model, which can accurately predict the properties of the laboratory-sized LSP, is needed in order to fill the gap between the laboratory-sized LSP and the larger LSP that would be required for a practical propulsion device.

Since the LSP has highly nonlinear thermodynamic, transport, and optical properties and an extremely large absorption of laser energy by the flow, a solution of this problem is not easily achieved. The modeling of the LSP began with the one-dimensional work of Raizer.⁷ Several other studies⁸⁻¹⁰ followed this analysis, but used more sophisticated analytical and computational methods. Unfortunately, one-dimensional models have an inherent weakness. The LSP tends to be highly dependent on laser beam geometry, radial convection, and radial diffusion transport of momentum and energy in the flow. Keefer and his co-workers^{11,12} developed a simplified semi-two-dimensional model that considered the radial energy diffusion, but assumed that the laser beam and the streamlines were parallel. Later, Glumb and Krier¹³ extended that model by using a converging laser beam as well as more realistic gas properties. However, their model still did not consider the momentum equations, but instead assumed a known velocity field. Merkle and his co-workers^{14,15} used a contemporary numerical method to attack the full two-dimensional problem. They succeeded in the calculation of a low-temperature LSP (peak temperature about 4000 K) in a hydrogen flow seeded with cesium. It is feasible to extend their approach to a pure hydrogen plasma,

Presented as Paper 86-1078 at the AIAA/ASME Fourth Fluid Mechanics, Plasma Dynamics and Lasers Conference, Atlanta, GA, May 12-14, 1986; received May 21, 1986; revision received Jan. 27, 1987. Copyright © American Institute of Aeronautics and Astronautics, Inc., 1986. All rights reserved.

*Assistant Professor, Mechanical and Aerospace Engineering, Center for Laser Applications. Member AIAA.

†Professor, Engineering Science and Mechanics, Center for Laser Applications. Member AIAA.

‡Predoctoral Fellow, Center for Laser Applications (presently Member of the Technical Staff, The Aerospace Corporation, El Segundo, CA). Student Member AIAA.

§Professor, Mechanical and Aerospace Engineering, Center for Laser Applications. Member AIAA.

but the higher peak temperature (about 16,000 K) and much stronger nonlinear optical properties of the pure hydrogen and argon plasma can result in numerical stability problems.

Recently, Jeng and Keefer¹ obtained a numerical solution for a rigorous two-dimensional model with realistic gas properties for the LSP in an argon flow. Their results agree well with the experimental data^{2,3} in the prediction of plasma position, size, shape, and peak temperature. Jeng and Keefer⁴ have also studied the effect of laser power, flow rate, static pressure, and optical geometry on the hydrogen LSP. They found that the zero radial velocity assumption used by Glumb and Krier¹³ is not adequate for this problem. Their work also indicated that there are no fatal errors in the laser propulsion concept and that the critical parameters, e.g., plasma size, position, radiation heat loss, and energy conversion efficiency, can be controlled using an appropriate optical arrangement and a suitable flow configuration.

The purposes of this work were to evaluate the full two-dimensional laser-sustained plasma model developed by Jeng and Keefer¹ against experimental results from Welle et al.³ to compare this model prediction with that from the constant axial mass flux, zero radial velocity, laser-sustained plasma model proposed by Glumb and Krier¹³ (referred to in this paper as the "quasi-two-dimensional" model), and to explore possible future model improvement. In the following section, the theoretical method used in the study is briefly described. This is followed by discussions of model calculations and of comparisons between the model calculations and experimental results. Additional details concerning the theoretical method can be found in Ref. 1.

Theoretical Model

The object of this work was the verification of the full two-dimensional model, and the simple flow geometry as shown in Fig. 1 was adopted. The domain is axisymmetric, and a cylindrical coordinate system was employed in the model. The argon enters from the bottom with a uniform velocity and temperature distribution and an originally collimated 10.6 μm CO₂ annular laser beam is focused into the gas by an appropriate lens.

It is assumed that the flow is laminar, low Mach number, steady state and axisymmetric and has variable thermo-physical and optical properties. The pressure of the flow is relatively high, so that local thermodynamic equilibrium (LTE) can be assumed with little error. Therefore, the plasma can be described by a single temperature and its intrinsic properties are only a function of this temperature and pressure. Thermal radiation is divided into two parts: an optically thin portion in which all radiation escapes from the plasma and an optically thick portion that can be described as a diffusion process. Since the Mach number for the flow is small, the kinetic energy and viscous dissipation are neglected in the energy equation. Following these assumptions, the equations of conservation of mass, momentum, and energy for the flow can be written as

$$\frac{\partial(\rho u)}{\partial x} + \frac{1}{r} \frac{\partial(r \rho v)}{\partial r} = 0 \quad (1)$$

$$\begin{aligned} \frac{\partial(\rho u u)}{\partial x} + \frac{1}{r} \frac{\partial(r \rho u v)}{\partial r} = & -\frac{\partial p}{\partial x} - \rho g \\ & + \left[\frac{\partial}{\partial x} \left(\mu \frac{\partial u}{\partial x} \right) + \frac{1}{r} \frac{\partial}{\partial r} \left(\mu r \frac{\partial u}{\partial r} \right) \right] \end{aligned} \quad (2)$$

$$\begin{aligned} \frac{\partial(\rho u v)}{\partial x} + \frac{1}{r} \frac{\partial(r \rho v v)}{\partial r} = & -\frac{\partial p}{\partial r} \\ & + \left[\frac{\partial}{\partial x} \left(\mu \frac{\partial v}{\partial x} \right) + \frac{1}{r} \frac{\partial}{\partial r} \left(\mu r \frac{\partial v}{\partial r} \right) \right] - \frac{2 \mu v}{r^2} \end{aligned} \quad (3)$$

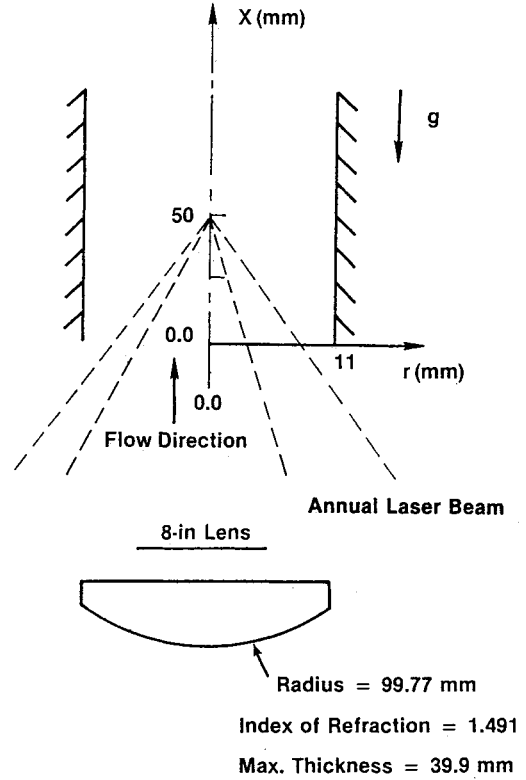


Fig. 1 Sketch of the test configuration.

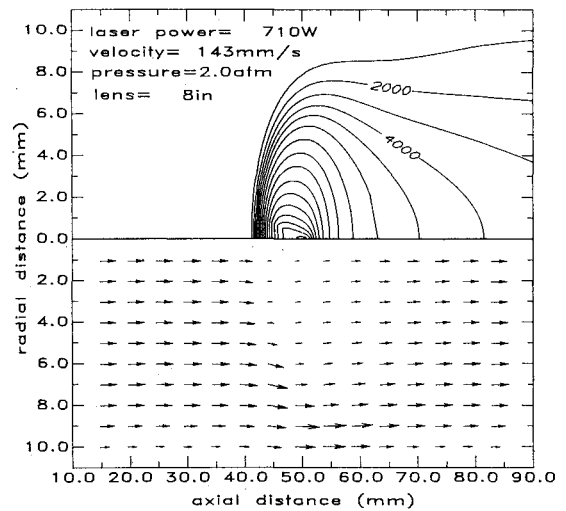


Fig. 2 Isothermal contour plot and mass flux vector plot of a calculated plasma (isothermal lines starting from 1000 K with 1000 K increments).

$$\begin{aligned} \frac{\partial(\rho u h)}{\partial x} + \frac{1}{r} \frac{\partial(r \rho v h)}{\partial r} = & \frac{\partial}{\partial x} \left(\frac{k_{\text{eff}}}{c_p} \frac{\partial h}{\partial x} \right) \\ & + \frac{1}{r} \frac{\partial}{\partial r} \left(\frac{r k_{\text{eff}}}{c_p} \frac{\partial h}{\partial r} \right) + \sum \alpha I_i - \dot{q}_{\text{rad}} \end{aligned} \quad (4)$$

where I_i is the local laser intensity described by

$$\frac{dI_i}{ds_i} = -\alpha I_i \quad (5)$$

and s_i is the distance along the laser ray propagation direction. The laser beam path through the optical system was

calculated by geometric ray tracing. The diffraction of the laser beam due to the finite aperture of the lens and the effects due to the inhomogeneous refractive index within the plasma are neglected in the calculations.

In Eqs. (2) and (3), the viscous term related to dilation has been omitted for computational efficiency. A few computations were made with the dilation term included and the influence of this term on the computed flowfield was found to be negligible.

The following properties of argon were used in the analysis. Thermodynamic properties (enthalpy, specific heat at constant pressure, and density) were interpolated from the tabulated values given by Drellishak et al.¹⁶ The viscosity between 5000 and 20,000 K was obtained from De Veto^{17,18} and below 5000 K the viscosity was interpolated from the graph given by Vargaftik and Filippov.¹⁹ The value of the intrinsic thermal conductivity for temperatures above 5000 K was adopted from De Veto^{17,18} and for the low temperature region, it was obtained from Vargaftik.²⁰ The absorption coefficient at 10.6 μm was calculated using the expression given by Kemp and Lewis,²¹ whose analysis included photoionization as well as electron-ion and electron-neutral inverse Bremsstrahlung using the Gaunt factors given by Karzas and Latter.²² The expressions for radiation loss were obtained from Kozlov et al.,²³ who considered both line and continuum emission in the optically thin limit as a function of temperature and density.

The use of the diffusion approximation for the radiation transport is not trivial; it is not a gas property and it depends upon the actual size and detailed temperature field of the plasma. If, according to the study of Kopainsky,²⁴ the size of the argon plasma is greater than 5 mm and the pressure is higher than 3 atm, then the radiation contribution below 200 nm represents a true optically thick case and the radiation-induced thermal conductivity no longer depends on the size of the plasma. The size and pressure of the plasmas under consideration are comparable to these limits. The theoretically calculated value of radiation-induced thermal conductivity²⁴ was used for static pressures greater than 3 atm, and an interpolated value between the experimental results²⁵ at 1 atm and the theoretical calculations²⁴ at 3 and 5 atm were used for low-pressure (<3 atm) flows.

Finite-Difference Solution

The finite-difference solution procedure employed in this work is an adaptation of the method described in detail by Patankar.²⁶ The detailed description of the numerical procedure used in the current calculations is discussed by Jeng

and Keefer¹ and only a brief description is presented in this section. The SIMPLE^{26,27} algorithm, which uses a conservative form of finite-difference equation, primitive variables, and staggered grids, was adopted to solve the coupled mass, momentum, and energy conservation equations [Eqs. (1-4)].

At a temperature of 300 K, argon is transparent to the laser irradiation, and the flow will absorb no energy. If the numerical calculation starts with a 300 K initial temperature distribution, a flow with uniform 300 K temperature will result. This solution is trivial and no plasma will be predicted. To obtain a (stable) LSP, an initial high-temperature zone around the focal point was assigned (resembling a spark ignition) where the size, position, and temperature of the "spark" were chosen by trial and error.

The computer code used in this study is similar to that of Jeng et al.^{1,4} Generally, the convergence of the numerical solution was achieved in 2000 iterations and the CPU time requirements are approximately 40 s for each iteration on a Masscomp-500 computer.

Results and Discussions

In the calculations, the wall and gas inlet temperature were assumed to be constant at 300 K and the inlet velocity to be uniform. The CO₂ laser operated at a wavelength of 10.6 μm and the collimated laser intensity distribution was that used by Jeng and Keefer.¹ It is an annular beam with peak intensity at a radius of 25.5 mm. The dimensions of the 8 in. focal length lens, which is one of two lenses used in the calculations, are shown in Fig. 1. Another lens of 12 in. focal length is similar to the 8 in. focal length lens, except for a maximum thickness of 39.9 mm and a radius of curvature of 143.2 mm.

The fundamental physical processes occurring within the LSP have been discussed by Jeng and Keefer.¹ The validity of the present model was established by calculations for two typical LSP's. The calculation included the interaction between the laser beam and the plasma, thermal radiation transport, and fluid convection. In the present paper, the verification of the model has been extended to a wider range of gas inlet velocities, gas static pressures, and laser power using two different lenses of 8 and 12 in. focal lengths. The flow conditions were varied at a static pressure of 1.3-4.0 atm, the flow inlet velocity at 0.4-4.5 m/s, and the laser power at 261-967 W.

Full Two-Dimensional and Quasi-Two-Dimensional Model Calculations

The temperature gradient within an LSP is very large, resulting in very high-density gradients and thus a very complex flow in the plasma. The most sophisticated quasi-two-dimensional model assumes a zero radial velocity, leading to a constant axial mass flux assumption. This simplifies the coupled nonlinear momentum and mass conservation differential equations so that the energy equation is the only differential equation to be solved numerically and the stability of the numerical solution is easily achieved. From the results of this work, the CPU time required for the quasi-two-dimensional model is at least of an order of magnitude less than that required for the full two-dimensional model. Figure 2 shows a typical calculated plasma from the full two-dimensional model. The isotherms are shown in the top half of the figure and the mass flux vectors in the bottom half. The laser focal zone is located 50 mm from the inlet and the directions and the magnitudes of the local mass flux, at the vector origins, is proportional to the directions and lengths of the vectors. The detailed heat-transfer and momentum transfer mechanisms for this LSP have been discussed by Jeng and Keefer,¹ so only a brief discussion is presented here. The LSP is positioned near the laser focal zone, and the peak temperature is 16,390 K. In the high-temperature region, where the axial velocities were much larger than

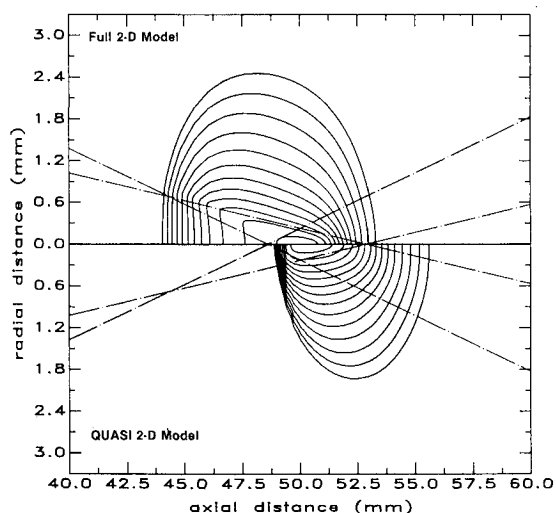


Fig. 3 Comparison of the calculated temperature contour between full two-dimensional and quasi-two-dimensional model (contour lines starting from 10,500 K with 500 K increments).

elsewhere, the axial mass flux was very small compared with the inlet mass flux. It was found that the plasma produced a local high-pressure zone near the leading edge of the plasma, which forced the flow to have outward radial velocities near the centerline. From this result, it is clear that the constant axial mass flux assumption in the quasi-two-dimensional model is inadequate.

A comparison of the temperature distribution calculated using the full two-dimensional and the quasi-two-dimensional models is shown in Fig. 3. The figure shows only a portion of the calculation domains near the laser focal zone and isotherms with temperature higher than 10,500 K. The innermost and outermost laser rays are also plotted in the figure. It was demonstrated in the earlier paper¹ that the calculations from the present model agreed well with the experimental data with regard to LSP position, size, and temperature distribution. The quasi-two-dimensional model, compared with the present model, predicts a smaller size for the plasma and a higher peak temperature. Although the location of the predicted maximum temperature is the same for both models, the detailed temperature distributions are considerably different. The quasi-two-dimensional model calculated a very steep temperature gradient and a short high-temperature zone upstream of the laser focal zone and most of the plasma was positioned downstream of the focal point. From the mass flux distribution shown in Fig. 2, it is clear that the quasi-two-dimensional model overestimated the axial mass flux in the high-temperature zone. In this case, the calculated plasma using the quasi-two-dimensional model is similar to the predictions that would be obtained with the full two-dimensional model having increased inlet velocity.

Model Verification

The model has been compared with a wide variety of experimental results given by Welle and his co-workers^{2,3} in order to learn the capability and limitations of the model. Since the spectroscopic measurements were limited to temperatures greater than 10,000 K, the following figures contain only those isotherms within that temperature range, and a limited portion of the calculation domain is plotted in order to gain a clearer comparison. Due to space limitations, only a few typical comparisons are presented in this section.

Inlet Velocity Effect

The performance of the model for two different inlet velocities, using the 8 in. focal length lens, is demonstrated in Figs. 4 and 5, respectively. The static pressure and laser power of these two LSP's differ by less than 1% and the inlet velocity of the LSP in Fig. 4 is about seven times that in Fig. 5. The model calculates the size and position of both plasmas well. As the inlet velocity increases, the radius of the plasma decreases, and the plasma is located further downstream. The local maximum temperatures within the low-velocity LSP are predicted by the model. One is on the laser path upstream of the focal zone and another is at the focal zone. Both calculated maximum temperatures are about 1000 K higher than the measured peak temperature (14,500 K). Only a single maximum temperature was measured, which was located neither on the laser path nor at the focal zone. The predicted local peak temperature at the focal zone, which was not observed in the experiment, may result from the neglect of the diffraction and refraction of the laser beam. Although it has been demonstrated experimentally^{2,3} that this assumption leads to only a small effect on the measured global laser power absorption, the predictive model can suffer more serious effects. If the refraction of the laser beam within the LSP is considered, it results in a larger focal spot size and reduced laser intensity. The spot size for the refracted beam is highly dependent on the LSP position and size. For a low-velocity LSP, most of the plasma is located upstream of the focal zone, making the focal spot larger. When diffraction is also considered, the

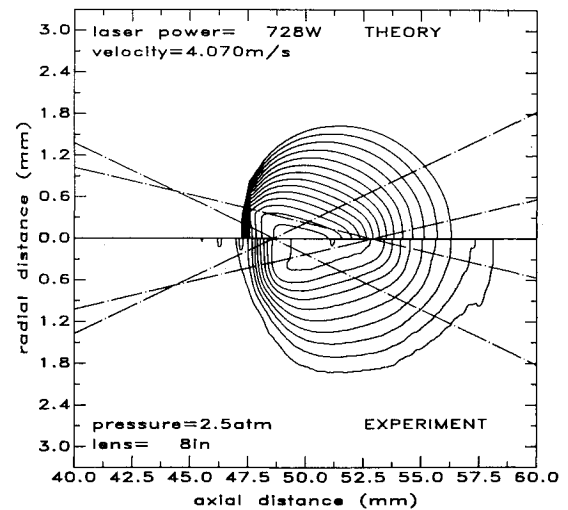


Fig. 4 Temperature contour plot of a high-velocity plasma (contour lines starting from 10,500 K with 500 K increments).

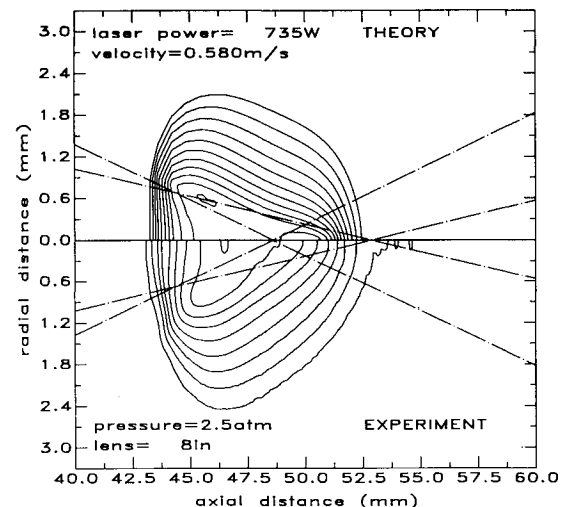


Fig. 5 Temperature contour plot of a low-velocity plasma (contour lines starting from 10,500 K with 500 K increments).

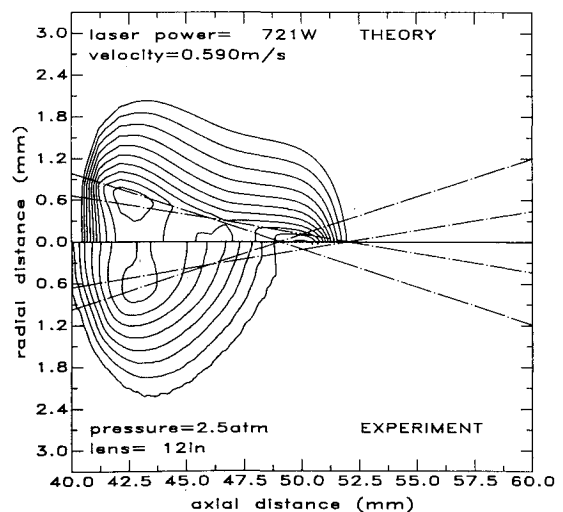


Fig. 6 Temperature contour plot of a low-velocity plasma with the 12 in. focal length lens (contour lines starting from 10,500 K with 500 K increments).

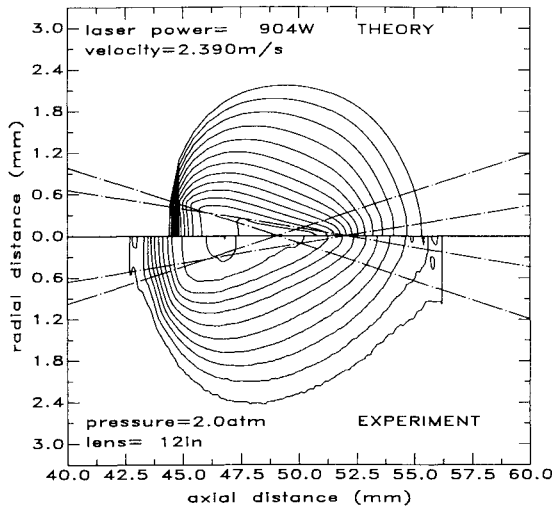


Fig. 7 Temperature contour plot of a plasma with high laser power (contour lines starting from 10,500 K with 500 K increments).

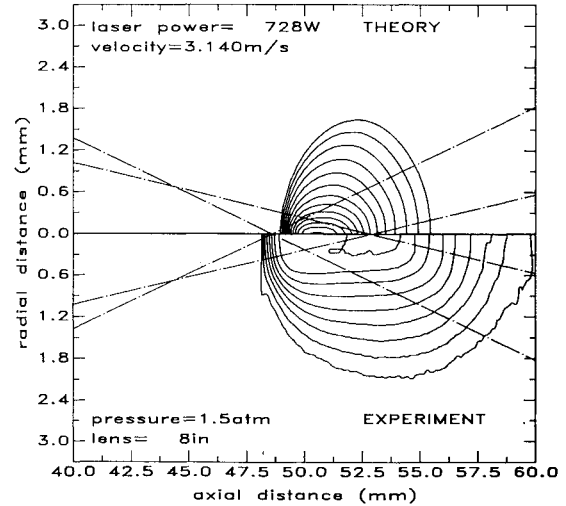


Fig. 9 Temperature contour plot of a low-pressure (1.5 atm) plasma (contour lines starting from 10,500 K with 500 K increments).

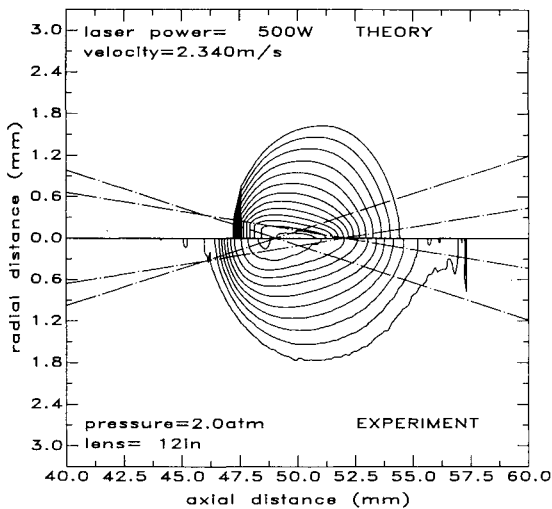


Fig. 8 Temperature contour plot of a plasma with low laser power.

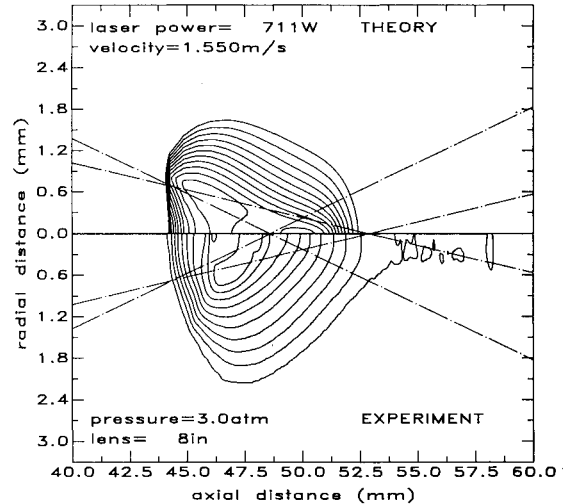


Fig. 10 Temperature contour plot of a high-pressure (3.0 atm) plasma (contour lines starting from 10,500 K with 500 K increments).

diffraction limited focal spot is approximately twice the size of that calculated from a geometric ray trace. The combination of laser beam refraction and diffraction and the longer absorption pathlength ahead of the focal zone result in an actual laser intensity that is smaller near the laser focal zone than that which is predicted by the model. Thus, the local temperature maximum will not be generated there in the low-velocity LSP. This may explain why the calculations are not consistent with the experiments in this detail.

Since the size and temperature of these LSP were well predicted, it is not surprising that the calculated thermal radiation power loss (316 and 445 W for high- and low-velocity, respectively) agreed with the experimental results (326 and 392 W for high- and low-velocity, respectively). The model prediction for the transmitted laser power in the high-velocity LSP also agrees reasonably well (110 and 159 W for prediction and experiment, respectively). However, the predicted transmitted laser power (91 W) in the low-velocity LSP is much smaller than the measurement (246 W). This is because the predicted second local maximum temperature near the focal zone absorbs an unrealistically large amount of additional laser power.

Lens Effect

Isotherms are shown in Fig. 6 for an LSP with operating conditions similar to those of Fig. 5 except for the use of the

12 in. focal length lens instead of the 8 in. lens. Both calculation and experiment show that the plasma moves further upstream than in Fig. 5 and the model predicted the upstream position and the radius of the plasma well. Again, the model predicts a local maximum temperature near the focal zone, which was not measured in the experiment. The effect of laser beam refraction and diffraction, which was discussed in the last section, is probably responsible. Similar to the 8 in. LSP, the thermal radiation from the LSP is well predicted and the transmitted laser power is underestimated.

Laser Power Effect

Figures 7 and 8 show the effect of laser power on the structure of the plasma. Both cases use the 12 in. focal length lens with similar flow conditions. The calculations are quite consistent with the experiments. As laser power increases, the plasma becomes larger and moves upstream. For the 10,500 K isotherms, the model underpredicted the length. However, the experimental results exhibit more noise in these isotherms than in the higher-temperature isotherms; if the 11,500 K isotherms are used, then the model predicts the length of this isotherm within 10%. The calculated positions of both plasmas are about 1 mm downstream of the experiments. After carefully reviewing the experimental data, it

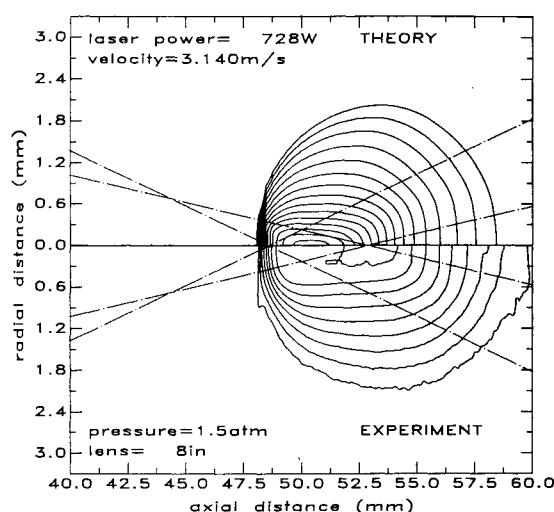


Fig. 11 Temperature contour plot of a low-pressure (1.5 atm) plasma using 50% of radiation-induced thermal conductivity (contour lines starting from 10,500 K with 500 K increments).

was found that the on-axis maximum temperatures are not on the laser beam path (using real ray tracing and neglecting the inhomogeneous refractive index effect). If the experimental results are shifted downstream by 1 mm, which is within the accuracy claimed by Welle et al.,³ the peak temperatures are located on the laser path. In this case, the model predictions agree well with the experimental LSP positions. The predicted global properties are also in reasonable agreement with the experiments: the transmitted laser power is within 10%, and the thermal radiation from the LSP is under-predicted within 30%.

Static Pressure Effect

All the LSP's shown in the previous sections have either 2.0 or 2.5 atm static pressure and the model performed well at these pressures. In this section, the effects of the static pressure are presented. The intrinsic properties of plasmas are highly pressure dependent, especially the optical properties. The absorption coefficient of the plasma at the laser wavelength and the thermal radiation from the plasma are approximately proportional to $p^{1.5}$. Figures 9 and 10 show the plasmas at 3.0 and 1.5 atm, respectively. Both plasmas have similar laser power levels and inlet mass flow rates (but different inlet velocities). In the low-pressure case, the predicted plasma size is much smaller than the experiment. In the 3 atm case, the model provides an excellent prediction.

After reviewing the model assumptions, we concluded that the treatment of the optically thick thermal radiation was the weakest link and was probably responsible for the failure of the model in the low-pressure case. As mentioned before, the validity of the diffusion approximation for short-range radiation is dependent on pressure and the size of the plasma. As the pressure decreases, the required size of the plasma increases. For the present calculation, the size of the 1.5 atm plasma is below the minimum size required for the valid use of the diffusion approximation found by Kopainsky.²⁴ Although the diffusion approximation for short-range thermal radiation is not valid for the low-pressure plasma, a sensitivity study using this approximation was performed to investigate the sensitivity of the solutions to radiative transport. For small, low-pressure plasmas, the radiation-induced thermal conductivity should be smaller than that for a large, low-pressure plasma.

A calculated result, where the radiation-induced thermal conductivity was reduced to 50% of the value used for the calculation in Fig. 9, is illustrated in Fig. 11. The size of this

plasma is much larger than the previous calculation and agrees well with the experimental results. The role of a change in thermal conductivity on the results can be understood qualitatively. As conductivity decreases, the conduction heat-transfer loss from the portion of the plasma along the laser path is reduced, which increases the plasma temperature along the laser path. Due to this increased temperature, the absorption coefficient at the laser wavelength increases and the plasma absorbs more laser power, which in turn generates a larger plasma. Because the exact solution of radiation heat transport will not be easy to achieve in the near future, the optically thin and thick approximations for the radiative transport process should be retained for the near term. Although in some pressure and dimension ranges the optically thick approximation is not quite valid, this concept can still be utilized with some adjustment for the magnitude of the radiation-induced thermal conductivity.

Conclusions

A full two-dimensional model for laser-sustained plasmas has been numerically solved for a wide range of argon flows. The calculations were compared with experimental temperature distributions and it was found that the model performed well at static pressures greater than 2 atm. The plasma position and size are well predicted and the behavior of the predicted plasma structure using different inlet velocity, focusing lenses, and laser power agreed well with experimental results.³

At lower pressures, the model underpredicts the plasma size. It was recognized that the diffusion approximation for short-range thermal radiation is probably responsible. When 50% of the optically thick, radiation-induced thermal conductivity at a pressure of 1.5 atm is used, the calculations are in reasonable agreement with experiments.

The global thermal radiation heat loss from the LSP and transmitted laser power are well calculated except for two LSP's. In these two LSP's, two local maximum temperatures were predicted. However, the experiment did not show the same two maxima. We concluded that neglecting the laser beam refraction and diffraction is responsible and recommend that the model should include these effects in future studies.

A comparison of calculations from the present model and those from a constant axial mass flux model was also performed. The axial mass flux field calculated from the present model differs considerably from the constant axial mass flux assumption in the simplified model. The characteristics of the temperature fields calculated with these two models are different and the results of the simplified model are similar to the calculated results from the present model using a much higher inlet velocity.

Acknowledgment

This work was partially supported by U.S. Air Force Office of Scientific Research Grant AFOSR-83-0043, the Program Manager was Dr. Robert Vondra.

References

- Jeng, S-M. and Keefer, D. R., "Theoretical Investigation of Laser-Sustained Argon Plasmas," *Journal of Applied Physics*, Vol. 60, Oct. 1986, pp. 2272-2279.
- Keefer, D. R., Welle, R. P., and Peters, C. E., "Power Absorption in Laser-Sustained Argon Plasmas," *AIAA Journal*, Vol. 24, Oct. 1986, pp. 1663-1669.
- Welle, R. P., Keefer, D. R., and Peters, C. E., "Laser-Sustained Plasmas in Forced Convective Argon Flow, Part I: Experimental Studies," *AIAA Journal*, Vol. 25, August 1987, pp. 1093-1099.
- Jeng, S-M. and Keefer, D. R., "Numerical Study of Laser-Sustained Hydrogen Plasmas in a Forced Convective Flow," *AIAA Paper 86-1524*, June 1986.

⁵Merkle, C. L., "Laser Radiation to Supply Energy for Propulsion," *AIAA Progress in Astronautics and Aeronautics: Orbit-Raising and Maneuvering Propulsion: Research Status and Needs*, Vol. 89, edited by L. H. Caveny, AIAA, NY, 1984, pp. 73-94.

⁶Keefer, D. R., Elkins, R., Peters, C., and Jones, L., "Laser Thermal Propulsion," *AIAA Progress in Astronautics and Aeronautics: Orbit-Raising and Maneuvering Propulsion: Research Status and Needs*, Vol. 89, edited by L. H. Caveny, AIAA, NY, 1984, pp. 129-148.

⁷Raizer, Y. P., "Subsonic Propagation of a Light Spark and Threshold Conditions for the Maintenance of Plasma by Radiation," *Soviet Physics—JETP*, Vol. 31, 1970, pp. 1148-1154.

⁸Jackson, J. P. and Nielsen, P. E., "Role of Radiative Transport in the Propagation of Laser-Supported Combustion Waves," *AIAA Journal*, Vol. 12, 1974, pp. 1498-1501.

⁹Kemp, N. H. and Root, R. G., "Analytical Study of Laser-Supported Combustion Waves in Hydrogen," *Journal of Energy*, Vol. 3, 1979, pp. 40-49.

¹⁰Keefer, D. R., Peters, C.E., and Crowder, H. L., "A Re-examination of the Laser Supported Combustion Wave," *AIAA Journal*, Vol. 23, 1985, pp. 1208-1212.

¹¹Batteh, J. H. and Keefer, D. R., "Two-Dimensional Generalization of Raizer's Analysis for the Subsonic Propagation of Laser Sparks," *IEEE Transactions on Plasma Science*, Vol. PS-2, 1974, pp. 122-129.

¹²Keefer, D. R., Crowder, H. L., and Elkins, R., "A Two-Dimensional Model of the Hydrogen Plasma for a Laser Powered Rocket," *AIAA Paper 82-0404*, Jan. 1982.

¹³Glumb, R. J. and Krier, H., "A Two-Dimensional Model of Laser-Sustained Plasmas in Axisymmetric Flowfields," *AIAA Paper 85-1553*, July 1985.

¹⁴Merkle, C. L., Molvik, G. A., and Choi, Y.-H., "A Two-Dimensional Analysis of Laser Heat Addition in a Constant Absorptivity Gas," *AIAA Journal*, Vol. 23, 1985, pp. 1053-1060.

¹⁵Merkle, C. L., Molvik, G. A., and Shaw, E. J.-H., "Numerical Solution of Strong Radiation Gasdynamic Interactions in a

Hydrogen-Seedant Mixture," *AIAA Paper 85-1554*, July 1985.

¹⁶Drellishak, K. S., Aeschliman, D. P., and Cambel, A. B., "Tables of Thermodynamics Properties of Argon, Nitrogen, and Oxygen Plasmas," *AEDC-TR-64-12*, 1964.

¹⁷DeVoto, R. S., "The Transport Properties of a Partially Ionized Monatomic Gas," Ph.D. Thesis, Stanford University, Stanford, CA, 1965.

¹⁸DeVoto, R. S., "Transport Properties of Ionized Monatomic Gases," *The Physics of Fluids*, Vol. 165, 1973, pp. 615-623.

¹⁹Vargaftik, N. B. and Filippov, L. P., *Thermal Conductivity of Gases and Liquids (Data Book)*, Standards Press, Cincinnati, 1970.

²⁰Vargaftik, N. B., *Tables on the Thermophysical Properties of Liquids and Gases*, Hemisphere Publishing, Washington, DC, 1975.

²¹Kemp, N. H. and Lewis, P. F., "Laser-Heated Thruster Interim Report," *NASA CR-161665*, 1980.

²²Karzas, W. J. and Latter, R., "Electron Radiative Transitions in a Coulomb Field," *Astrophysical Journal Supplement Series*, Supp. 55, Vol. VI, May 1961.

²³Kozlov, G. I., Kuznetsov, V. A., and Masyukov, V. A., "Radiative Losses by Argon Plasma in the Emissive Model of a Continuous Optical Discharge," *Soviet Physics—JETP*, Vol. 39, 1974, pp. 463-468.

²⁴Kopainsky, J., "Strahlungstransportmechanismus und Transportkoeffizienten im Ar-Hochdruckbogen," *Zeitschrift für Physik*, Vol. 248, 1971, pp. 417-432.

²⁵Bues, J., Patt, H. J., Richter, J., "Über die Elektrische Leitfähigkeit und die Wärmeleitfähigkeit des Argons bei Hohen Temperaturen," *Zeitschrift für Angewandte Physik*, Vol. 22, 1967, p. 345.

²⁶Patankar, S. V., *Numerical Heat Transfer and Fluid Flow*, Hemisphere Publishing, Washington, DC, 1980.

²⁷Gosman, A. D., Pun, W. M., Ruchal, A. K., Spalding, D. B., and Wolfshstein, R., *Heat and Mass Transfer in Recirculating Flows*, Academic Press, London, 1969.

From the AIAA Progress in Astronautics and Aeronautics Series

THERMOPHYSICS OF ATMOSPHERIC ENTRY—v. 82

Edited by T.E. Horton, The University of Mississippi

Thermophysics denotes a blend of the classical sciences of heat transfer, fluid mechanics, materials, and electromagnetic theory with the microphysical sciences of solid state, physical optics, and atomic and molecular dynamics. All of these sciences are involved and interconnected in the problem of entry into a planetary atmosphere at spaceflight speeds. At such high speeds, the adjacent atmospheric gas is not only compressed and heated to very high temperatures, but strongly reactive, highly radiative, and electronically conductive as well. At the same time, as a consequence of the intense surface heating, the temperature of the material of the entry vehicle is raised to a degree such that material ablation and chemical reaction become prominent. This volume deals with all of these processes, as they are viewed by the research and engineering community today, not only at the detailed physical and chemical level, but also at the system engineering and design level, for spacecraft intended for entry into the atmosphere of the earth and those of other planets. The twenty-two papers in this volume represent some of the most important recent advances in this field, contributed by highly qualified research scientists and engineers with intimate knowledge of current problems.

Published in 1982, 521 pp., 6×9, illus., \$35.00 Mem., \$55.00 List

TO ORDER WRITE: Publications Order Dept., AIAA, 370 L'Enfant Promenade, SW, Washington, DC 20024